

Electron-irradiation-induced deep levels in *n*-type 6H-SiC

M. Gong, S. Fung,^{a)} and C. D. Beling

*Department of Physics, The University of Hong Kong, Pokfulam Road, Hong Kong,
The People's Republic of China*

Zhipu You

Department of Physics, Sichuan University, Chengdu, Sichuan 610064, The People's Republic of China

(Received 9 December 1998; accepted for publication 2 March 1999)

The fluence-dependent properties and the annealing behavior of electron-irradiation-induced deep levels in *n*-type 6H-SiC have been studied using deep-level transient spectroscopy (DLTS). Sample annealing reveals that the dominant DLTS signal at $E_C - 0.36$ eV (labeled as *E1* by others) consists of two overlapping deep levels (labeled as ED_{3L} and ED_{3H}). The breakup temperature of the defect ED_{3L} is about 700 °C. The ED_{3H} center together with another deep level located at $E_C - 0.44$ eV (so-called *E2*) can withstand high-temperature annealing up to 1600 °C. It is argued that the involvement of the defect ED_{3L} is the reason that various concentration ratios of *E1/E2* were observed in the previous work. The revised value of the capture cross section of the deep-level ED_{3H} has been measured after removing ED_{3L} by annealing. A deep level found at $E_C - 0.50$ eV is identified as a vacancy-impurity complex since it was found to have a lower saturated concentration and weak thermal stability. Two other deep levels, $E_C - 0.27$ eV and $E_C - 0.32$ eV, which were not observed by others because of the carrier freeze-out effect, are also reported. © 1999 American Institute of Physics. [S0021-8979(99)07911-6]

I. INTRODUCTION

Silicon carbide (SiC) holds great potential value as a semiconductor material for power devices since it can retain its properties under extreme conditions, one of which is an ionizing radiation environment. In addition, ion implantation has become a key technique in the manufacture process since it is the only viable method to realize selective area doping on SiC. Unfortunately, however, there is always some radiation-induced damage remaining in the operational area of the device even after an annealing procedure. It is, therefore, important to reveal the nature of irradiation-induced defects or damage. High-energy electron irradiation is widely used to study the defects in semiconductors since it is a controllable way to introduce intrinsic defects and complex centers, and as such, can be used to illuminate some properties of the defects. In past years, many results have been obtained for electron irradiation defects in 6H-SiC using various methods.¹⁻⁹ The present work seeks to complement them.

The influence of a defect on the electrical properties of the material is generally evaluated through the deep level that it introduces. For this reason, the deep-level transient spectroscopy (DLTS) technique has been employed to monitor the behavior of the electron irradiation-induced deep levels in SiC.⁷⁻⁹ Some deep levels, including the *Z1/Z2*, *E1/E2*, and *E3/E4* centers monitored using DLTS in electron-irradiated *n*-type 6H-SiC, were first reported by Zhang *et al.*⁷ Among these, the *E1/E2* centers were dominant. These defects always appear in pairs in DLTS spectra and are thus considered to be due to the defects that reside at

inequivalent lattice sites.¹⁰ Recently, a new DLTS peak, situated at $E_C - 0.51$ eV and having a greater concentration than those typical of the *Z1/Z2* center, has been observed in electron-irradiated 6H-SiC.^{8,9}

With regard to the defect microstructure, it has been suggested that the *Z1/Z2* centers are simply the divacancy ($V_C - V_{Si}$) observed using electron-spin resonance (ESR) (Ref. 11) and equates with the *D1* center measured using photoluminescence (PL),² the reason for this association is solely that these signatures all withstand heat treatments up to 1700 °C.^{10,12} On the other hand, the generation rate of the *Z1/Z2* centers varies considerably from sample to sample as observed in different studies, even though the electron-beam energies were similar (in the range 2–2.5 MeV).^{9,10} The structure of the dominant defects *E1/E2*, which occupy inequivalent lattice sites, are still unclear and the ratio of their DLTS peaks are also different from sample to sample.⁸⁻¹⁰ Thus, in spite of extensive studies, the physical identity of the irradiation-induced deep levels in SiC remains largely unknown.

In the present work, the DLTS technique has been employed to study the electron-irradiation-introduced deep-level defects in *n*-type 6H-SiC. Several deep levels are distinguished and some information is revealed from the electron-beam fluence-dependent properties and the annealing behavior of the deep levels.

II. EXPERIMENT AND RESULTS

The *n*-type 6H-SiC used in this experiment was obtained from CREE Research, Inc. The (0001)-oriented wafer had a basic nitrogen (N) dopant concentration of $1.0 \times 10^{18} \text{ cm}^{-3}$ with a chemical-vapor deposition (CVD) grown

^{a)}Electronic mail: sfung@hkucc.hku.hk

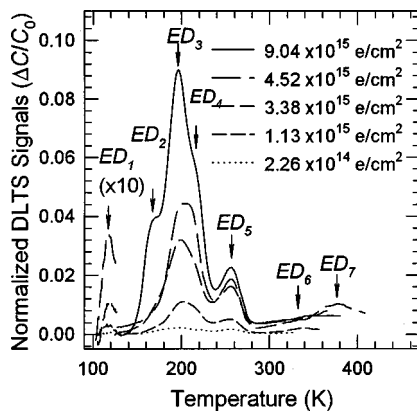


FIG. 1. Normalized DLTS spectra of electron-irradiated *n*-type 6H-SiC with various electron-beam fluences. The rate window used in the measurement is 6.82 ms.

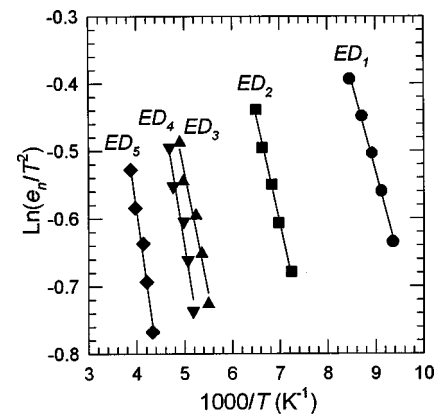


FIG. 2. Arrhenius plots of electron emission rates as a function of $1000/T$, for the electron-irradiation-induced deep levels in *n*-type 6H-SiC. The energy positions are $ED_1: E_C - 0.27$ eV; $ED_2: E_C - 0.32$ eV; $ED_3: E_C - 0.36$ eV; $ED_4: E_C - 0.44$ eV; and $ED_5: E_C - 0.50$ eV, respectively.

epilayer of 10 μm thickness of $1.3 \times 10^{16} \text{ cm}^{-3}$ nitrogen dopant concentration. Ni-SiC ohmic contacts on the rough (substrate) sides of the samples were manufactured by annealing the Ni contact at 950 °C for 5 min in mixed gas of high-purity-grade nitrogen (80%) and hydrogen (20%) before electron irradiation. The samples were irradiated using a 1.7 MeV electron-beam produced in a linear accelerator. The fluence of the implanted electrons was varied from 2.26×10^{14} to $9.04 \times 10^{15} \text{ e/cm}^2$. Unirradiated control samples were also made to check if any native deep centers existed in the material. After irradiation, gold (Au) was deposited on the frontside (epilayer) of the samples in a vacuum of $\sim 10^{-6}$ Torr to form a Schottky barrier. During all the above preparation procedures, the temperatures of the samples were not higher than 80 °C. The quality of all the Schottky-diode-like samples was monitored by observing the current-voltage (I - V) and the capacitance-voltage (C - V) characteristics.

Some typical DLTS spectra of *n*-type 6H-SiC with various electron-beam fluences are presented in Fig. 1. While there are no deep-level signals in the unirradiated control sample, at least seven DLTS peaks are observed in the irradiated samples in the temperature region from 100 to 400 K. They are labeled as ED_1 , ED_2 , ED_3 , ED_4 , ED_5 , ED_6 , and ED_7 (here, ED means electron-beam-induced donor trap), in which ED_3 and ED_4 are dominant. The positions of the deep levels in the band gap, as determined by the Arrhenius plots shown in Fig. 2, are $ED_1: E_C - 0.27$ eV; $ED_2: E_C - 0.32$ eV; $ED_3: E_C - 0.36$ eV; $ED_4: E_C - 0.44$ eV; and $ED_5: E_C - 0.50$ eV, respectively. Since the amplitudes of peaks ED_6 and ED_7 are too small, it was not possible to obtain reliable positions for these levels. Since no deep level was observed in the control sample and the observed deep levels ED_1 - ED_5 in irradiated samples are obviously dependent on the electron dose, it may be concluded that all of these levels (except ED_6 and ED_7) are due to the electron irradiation.

It is noted that both the positions ($E_C - 0.36$ eV, and $E_C - 0.44$ eV) and the capture cross sections (2.7×10^{-15} and $8.6 \times 10^{-14} \text{ cm}^2$, as calculated from the Arrhenius plots in Fig. 2 of ED_3 and ED_4) are very close to those of the defects $E1/E2$, as observed in previous DLTS studies.⁷⁻⁹ This leads

us to believe that the defects ED_3/ED_4 in the present work are indeed the defects $E1/E2$ as seen by others. Deep-level ED_5 at $E_C - 0.50$ eV with capture cross section $1.7 \times 10^{-14} \text{ cm}^2$ did not appear in the DLTS spectra of the earlier work.⁷ It has, however, been repeatedly observed in recent experiments such as in Refs. 8 and 9. In the lower-temperature region of the DLTS spectra, the two electron-irradiation-induced defects ED_1 and ED_2 have not been reported in any previous works to the best of our knowledge.⁷⁻⁹ The deep center ED_1 was only observed in the samples with low fluence electron irradiation as shown in Fig. 1.

In the higher-temperature region of the DLTS spectra, we can see several small signals (referred to here as ED_6 and ED_7), which overlap each other. Compared to the previously results,^{7,9} these levels could possibly be identified with defects $E3/E4$ and $Z1/Z2$. However, the intensity of ED_6 and ED_7 does not depend on the irradiation dose. In addition, their amplitudes relative to the ED_3/ED_4 ($E1/E2$) levels in the DLTS spectra are much smaller than those of reported results,⁷ especially in the samples with higher electron dose as seen in Fig. 1.

Fluence-dependent properties are shown in Fig. 3. A low

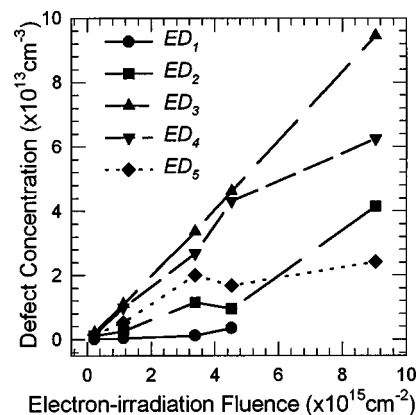


FIG. 3. Concentrations of the electron-irradiation-induced deep levels in *n*-type 6H-SiC as a function of electron-beam fluences.

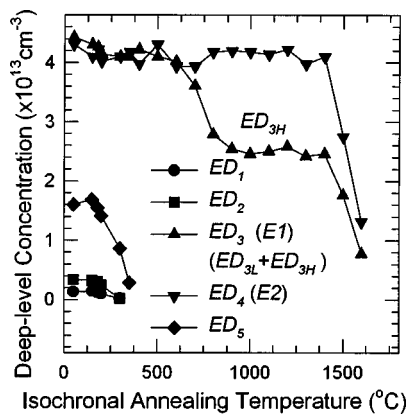


FIG. 4. Isochronal-annealing behavior of the deep levels measured from the sample irradiated to $4.52 \times 10^{15} \text{ e/cm}^2$.

saturated concentration of ED_5 is observed while the concentrations of the other defects increase with the electron-beam fluence. Figure 4 gives the 5 min isochronal-annealing behavior for the deep-level centers in electron-irradiated *n*-type SiC measured in this work. Defects ED_1 and ED_5 anneal out after 300 °C thermal treatment, while defects ED_3 and ED_4 can withstand a heating even as high as 1600 °C. Of particular interest is the two-stage annealing of ED_3 , the first stage occurring at 700 °C. No new DLTS peak was observed at any annealing stage.

III. DISCUSSION

A. ED_1 and ED_2

Since the two new deep levels ED_1 ($E_C - 0.27 \text{ eV}$) and ED_2 ($E_C - 0.32 \text{ eV}$) are electron-dose dependent, there is no doubt that they are associated with radiation-induced defects. In the heavily ($9.04 \times 10^{15} \text{ e/cm}^2$) irradiated sample, we could not observe these two defects. This is due to the carrier freeze-out effect caused by the strong compensation of the dopant and the high concentration of radiation-induced defects at low temperature. The plots “a” and “b” in Fig. 5 show the temperature-dependent Schottky barrier capacitance of the samples with 3.38×10^{15} and $9.04 \times 10^{15} \text{ e/cm}^2$, respectively. It is noted that the capacitance of the more heavily irradiated sample approaches zero in the temperature region below 150 K, while that of the lightly irradiated sample remains higher until 100 K. This result indicates that a strong compensation is indeed occurring in the more heavily irradiated sample. It is confirmed in plot “c” in Fig. 3, which shows the DLTS signals for this sample falling in the temperature region of carrier freeze-out. It is probable that ED_1 and ED_2 have not been observed by other authors for the same reason,⁷⁻⁹ although, since no mention was made of any compensating effect, it is difficult to be certain of this. If, on the other hand, the freeze-out effect did not occur in these experiments, some unexpected impurity might have been involved. The extremely strong signal of ED_2 in the sample with $9.04 \times 10^{15} \text{ e/cm}^2$ irradiation, as shown in Fig. 1, may indicate the presence of some kind of impurity having inhomogeneous distribution. The low dissociation tempera-

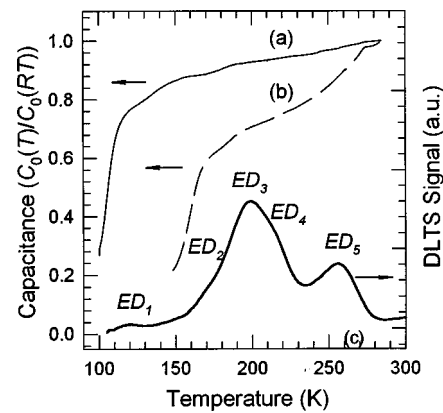


FIG. 5. The static capacitance (plots a and b) and the transient capacitance (DLTS, plot c) as a function of the substrate temperature to show the influence of the freeze-out effect on the transient capacitance (DLTS).

ture of ED_1 and ED_2 , as shown in Fig. 4, suggests that these levels may be interstitial or impurity related since an interstitial atom has a lower migration energy.

B. ED_3 and ED_4

The defects ED_3 and ED_4 , which have been called *E1/E2* by other authors,⁷⁻⁹ are commonly considered as the same defects occupying the hexagonal and cubic lattice sites, respectively. According to this model, the ratio of their concentrations should be fixed rather than varying from sample to sample. In our experiment, however, a large discrepancy exists. The DLTS spectra in Fig. 1 show that the ratio of ED_3 to ED_4 varies from sample to sample. The concentration of ED_3 increased linearly with the electron fluence, but the production rate of ED_4 decreases, as shown in Fig. 3. Similar phenomena were also observed by other authors,⁷⁻⁹ where the amplitude of *E2* was even larger than that of *E1*. These interesting results may indicate that either the deep levels, ED_3 and ED_4 , are not the same defects with inequivalent lattice sites or that there may be another deep level, with a similar energy and capture cross section that overlaps the DLTS peaks of ED_3 and ED_4 .

Both defects ED_3 and ED_4 have an annealing temperature of about 1600 °C, as shown in Fig. 4. As mentioned, however, the annealing process of ED_3 is divided into two stages. Part of the defects that produce the DLTS peak ED_3 , anneal out at 700 °C while the remainder, with a constant concentration, survive until up to 1600 °C, at which point defect ED_4 also dissociates. In the temperature region of 700–1600 °C, the concentration ratio of ED_3 to ED_4 remains constant. These aspects of defect ED_3 strongly support the suggestion that the DLTS peak of ED_3 is an overlap of two deep levels, which probably have very close energy levels and capture cross sections. Here, these two levels are labeled as ED_{3L} and ED_{3H} , ED_{3L} being that component stable below 700 °C and ED_{3H} the component stable to high temperature. The DLTS spectra of 1150 °C annealed samples with irradiation doses of 1.13×10^{15} and $9.04 \times 10^{15} \text{ e/cm}^2$, respectively, are presented in Fig. 6. The plots are normalized so that we can easily compare the two plots in detail. It is obvious that there is almost no difference between the two

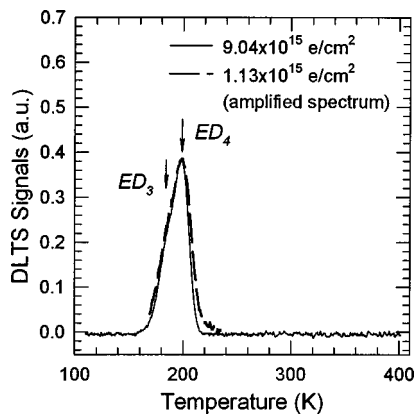


FIG. 6. DLTS spectra of samples irradiated to 4.52×10^{15} and 1.13×10^{15} e/cm^2 after $1150^\circ C$ annealing. The rate window used in the measurement is 54.56 ms.

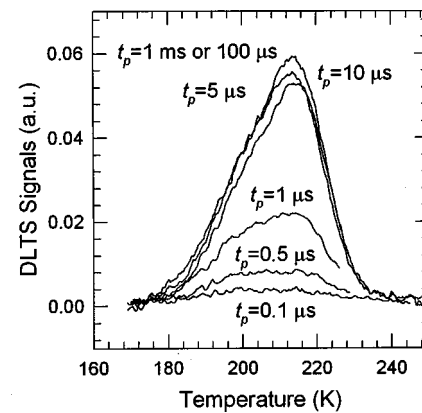


FIG. 7. DLTS spectra that were measured under the conditions of various filling pulse widths (t_p). The sample used in the measurement was annealed at $1150^\circ C$ after being irradiated to 1.13×10^{15} e/cm^2 .

plots. The final ratios of ED_{3H} to ED_4 in both samples after $1150^\circ C$ annealing are approximately equal to 0.6, which agrees well with the value (0.61) of Zhang *et al.* (Fig. 7 of Ref. 10). The constant concentration ratio of ED_{3H} to ED_4 and the same annealing temperature indicate that defects ED_{3H} and ED_4 are indeed the same defects occupying inequivalent lattice sites. The other part of ED_3 , named as ED_{3L} , with lower thermal stability is probably due to an impurity-related complex since its concentrations are different from sample to sample in Refs. 7–9 and this work. The annealing behavior of the ED_{3H}/ED_4 ratio is very similar to that of the defects monitored by positron annihilation spectroscopy,^{4–6} in which the defects having a positron lifetime of ~ 210 ps were annealed out at 1500 – $1700^\circ C$. These defects were suggested to have a structure of $(V_{Si} + V_C)$ divacancy according to the linear muffin-tin orbital atomic-sphere approximation (LMTO-ASA) calculation performed by Brauer *et al.*¹³

Recently, a further study on the capture cross sections of electron irradiation-induced deep levels in n -type 6H-SiC has been presented.⁹ The values of the measured capture cross sections are approximately 8.95×10^{-16} cm^2 for $E1$ and 7.27×10^{-17} cm^2 for $E2$, respectively. The electron capture ability of $E1$ is one order greater than that of $E2$. Since $E1/E2$ have been identified as the same kind of defects occupying inequivalent lattice sites, their physical parameters would not be expected to have such a large difference. In the Hemmingsson *et al.* experiment,⁹ the concentration of $E1$ (9.5×10^{13} cm^{-3}) is a little bit greater than that of $E2$ (8.8×10^{13} cm^{-3}). This is also suggestive of the involvement of another kind of defect, i.e., ED_{3L} . Therefore, the transient signal of $E1$ that was measured is larger than what it should be since it includes the contribution of ED_{3L} (see Fig. 5 of Ref. 9), especially in the short-filling pulse-width case. This result also indicates that ED_{3L} has the larger electron capture cross section. To test this hypothesis, the DLTS spectra in Fig. 7 are monitored by applying various widths of the filling pulse on the $1150^\circ C$ annealed sample, in which the defect ED_{3L} has been removed. It is obvious that the amplitude of ED_{3H} is always weaker than that of ED_4 and their ratio is approximately equal to 0.6, except in the case of

a very short-filling pulse width, in which case some surviving ED_{3L} may be still involved. The measured capture cross sections of ED_{3H} and ED_4 are 4.97×10^{-17} and 5.72×10^{-17} cm^2 , respectively. These values are very close to each other and agree well with the result (7.27×10^{-17} cm^2) of the $E2$ center measured by Hemmingsson *et al.*⁹

As mentioned above, both the high-temperature stability and positron lifetime results point to ED_{3H}/ED_4 being the $V_C - V_{Si}$ divacancy. However, this interpretation conflicts with the suggestion that the deep levels $Z1/Z2$ result from this divacancy, which also has high-temperature stability. In the higher-temperature region of the DLTS spectra presented in Fig. 1, several low-intensity deep-level peaks, which overlap one another, can be observed. One of them, ED_7 appears similar to the defects $Z1/Z2$ in the previous reports,^{7,9} due to its having a similar position (~ 400 K) in the spectra. The reported $Z1/Z2$ levels peak in the temperature region of 390 – 420 K in the DLTS spectra having a rate window of 4.33 ms.¹⁰ If a sample is measured with a larger rate window, its DLTS peaks will shift into a lower-temperature region. It would thus be expected to see the signals of $Z1/Z2$ appearing in the $1150^\circ C$ annealed spectra of Fig. 6, which was measured with a rate window of 54.56 ms. No DLTS signal, however, is observed in our spectra in the region of 250 – 400 K. This means that either the $Z1/Z2$ center does not exist in our samples or that defect $Z1/Z2$ can be annealed out at a temperature lower than $1150^\circ C$.

A high-temperature ($>1200^\circ C$) annealing experiment of the electron-beam-induced defects $Z1/Z2$ was performed a few years ago by Zhang *et al.*⁷ In their experiment, an incomplete DLTS spectrum (range 160 – 320 K), obtained after $1450^\circ C$ annealing, was presented (Fig. 7 in Ref. 10). A series of new large DLTS signals, not observed in their $1200^\circ C$ annealed sample but appearing in the region of 240 – 320 K after $1450^\circ C$ annealing, indicates that some new defects had been formed in their sample during the annealing process. There was, however, no indication of $Z1/Z2$ being present. Moreover, the existence of new deep centers with high concentration would likely lead to either the carrier freeze-out effect or alternatively result from impurity inter-

action. In both cases, the defect center $E1/E2$ would not be observed after 1450 °C annealing. In the former case, the defect center would still exist, supporting our present observation of $E1/E2$ up to 1600 °C annealing. That defects $Z1/Z2$ used to be considered as a complex of two adjacent vacancies ($V_C - V_{Si}$), which was observed using ESR,¹¹ is basically built on the observation of its high thermal stability rather than the direct measurement. However, the present experiment shows that defects $Z1/Z2$ do not exist after 1150 °C annealing. Instead, defects $ED_{3H}/ED_4(E1/E2)$ that can withstand 1600 °C annealing are the ones observed. In conclusion, it seems that ED_{3H}/ED_4 , but not $Z1/Z2$, is the defect center stable to 1600 °C, and thus, the ones associated with ($V_C - V_{Si}$).

C. ED_5

Figure 3 reveals that defect $ED_5(E_C - 0.50 \text{ eV})$ has a saturated concentration with increasing electron fluence. Since the relative amplitude of level ED_5 to ED_3 in the lightly irradiated sample is remarkably larger than that in the heavily irradiated one, as shown in Fig. 1, this phenomenon cannot be due to the experimental errors. This also cannot be caused by the carrier freeze-out effect since much larger influences on the shallower levels ED_3 and ED_4 would exist if this effect were occurring. The phenomenon of saturation, however, finds a natural explanation in terms of the interaction between an induced vacancy and some kind of original impurity. In this case, the differential production rate of ED_5 obeys the relation of

$$\left(\frac{\partial N_{ED_5}}{\partial D} \right) \propto (N_I - N_{ED_5}), \quad (1)$$

which leads to the general form

$$N_{ED_5} \propto N_I (1 - e^{-\alpha D}). \quad (2)$$

Here, α is a constant, N_{ED_5} is the concentration of defect ED_5 , D is the electron fluence, and N_I is the concentration of the impurity that acts with the vacancy to form the defect complex ED_5 . ED_5 has similar low-temperature annealing characteristics to ED_1 and ED_2 , as shown in Fig. 4, thus the impurity involved in the defect ED_5 may involve the interstitial site. Since an interstitial atom has a weak bonding to the nearest atom, the defects occupying inequivalent lattice sites would not be expected to introduce any significant energy difference. As a result, the defect ED_5 would appear as a single peak rather than as paired ones in the DLTS spectra, as is indeed observed for ED_1 and ED_2 . At this stage, however, it is impossible, using DLTS only, to know what the impurity is.

IV. CONCLUSIONS

In conclusion, we have studied the electron irradiation-induced deep-level defect centers in *n*-type 6H-SiC using deep-level transient spectroscopy. Two electron-irradiation-induced deep levels ED_1 and ED_2 , which are located at 0.27

and 0.32 eV below the conduction band, respectively, have been found in the samples with low fluence irradiation. The reason that these deep levels were not observed by other researchers has been suggested as due to the carrier freeze-out effect. From the available information, it is difficult to deduce the structure of the defects ED_1 and ED_2 . By analyzing the electron-beam fluence-dependent properties and annealing behaviors of the deep levels, some information has been revealed. The most important finding is that defect ED_{3L} has been distinguished from the overlapping $E1$ signal. The presence of this defect makes the concentration ratio of $E1/E2$ variable and leads to the large variations found in this ratio in the literature. The dominant defects ED_{3H}/ED_4 (or $E1/E2$) are confirmed to be the same defects occupying inequivalent lattice sites. These two deep levels have not only very close energy positions but also have very close electron capture cross sections, the same annealing behaviors, and a fixed ratio of concentrations. Since the deep levels $Z1/Z2$ were not observed in this work, there is still a strong suspicion against the model that defects $Z1/Z2$ are divacancies ($V_C - V_{Si}$). Indeed, the $E1/E2$ (ED_{3H}/ED_4) centers are far more likely candidates for a structure based on ($V_C - V_{Si}$), as they have more certain high-temperature annealing properties. Defect ED_5 has also been observed and has been suggested to be a vacancy-impurity complex as a result of its observed lower saturated concentration and weak thermal stability. To illuminate the structures of the electron-irradiation-induced defects, further studies of their annealing behavior, using DLTS combined with PL, ESR, and positron annihilation techniques, will be necessary.

ACKNOWLEDGMENTS

One of the authors (S.F.) wishes to acknowledge valuable financial support from the HKU CRCG and Hong Kong RGC research grants.

- ¹L. A. de S. Balona and J. H. N. Loubser, *J. Phys. C* **3**, 2344 (1970).
- ²L. Patrick and W. J. Choyke, *Phys. Rev. B* **8**, 3253 (1972).
- ³N. T. Son, E. Sörman, M. Singh, W. M. Chen, C. Hallin, O. Kordina, B. Monemar, J. L. Lindström, and E. Janzén, *Diamond Relat. Mater.* **6**, 1378 (1997).
- ⁴A. A. Rempel and H. H. Schaefer, *Appl. Phys. A: Mater. Sci. Process.* **61**, 51 (1995).
- ⁵A. Kawasuso, H. Itoh, S. Okada, and H. Okumura, *J. Appl. Phys.* **80**, 5639 (1996).
- ⁶A. Kawasuso, H. Itoh, H. Okumura, K. Abe, and S. Okada, *J. Appl. Phys.* **82**, 3232 (1997).
- ⁷H. Zhang, G. Pensl, A. Dömen, and S. Leibenzeder, *The Electrochemical Society, Extended Abstract* **89-2**, 699 (1989).
- ⁸J. P. Doyle, M. O. Aboelfotoh, B. G. Svensson, A. Schöner, and N. Nordell, *Diamond Relat. Mater.* **6**, 1388 (1997).
- ⁹C. Hemmingsson, N. T. Son, O. Kordina, E. Janzén, and J. L. Lindström, *J. Appl. Phys.* **84**, 704 (1998).
- ¹⁰G. Pensl and W. J. Choyke, *Physica B* **185**, 264 (1993).
- ¹¹V. S. Vaïner and V. A. Il'in, *Sov. Phys. Solid State* **23**, 2126 (1981).
- ¹²T. Dalibor, C. Peppermüller, G. Pensl, S. Sridhara, R. P. Devaty, W. J. Choyke, A. Itoh, T. Kimoto, and H. Matsunami, *Inst. Phys. Conf. Ser.* **142**, 517 (1995).
- ¹³G. Brauer, W. Anwand, E. M. Nicht, J. Kuriplach, M. Sob, N. Wagner, P. G. Coleman, M. J. Puska, and T. Korhonen, *Phys. Rev. B* **54**, 2512 (1996).